Poisson-distributed Active Fusion Complexes Underlie the Control of the Rate and Extent of Exocytosis by Calcium

Steven S. Vogel, Paul S. Blank, and Joshua Zimmerberg

Laboratory of Theoretical and Physical Biology, National Institute of Child Health and Human Development, National Institutes of Health, Bethesda, Maryland 20892

Abstract. We have investigated the consequences of having multiple fusion complexes on exocytotic granules, and have identified a new principle for interpreting the calcium dependence of calcium-triggered exocytosis. Strikingly different physiological responses to calcium are expected when active fusion complexes are distributed between granules in a deterministic or probabilistic manner. We have modeled these differences, and compared them with the calcium dependence of sea urchin egg cortical granule exocytosis. From the calcium dependence of cortical granule exocytosis, and from the exposure time and concentration dependence of *N*-ethylmaleimide inhibition, we determined that cortical granules do have spare active fusion complexes that are randomly distributed as a Poisson process among the population of granules. At high calcium concentrations, docking sites have on average nine active fusion complexes.

Exocytosis involves many steps, including the biosynthesis of vesicles and their contents, vesicle transport to the plasma membrane, docking, the merging of membranes, and the release of vesicle contents. After exocytosis, there is often calcium-dependent granule mobilization (39) and endocytic membrane retrieval (48, 49). In sea urchin eggs, the cellular machinery that mediates membrane merger in calcium-triggered exocytosis, the fusion complex, resides on exocytotic granules (53) and can undergo conformational changes from inactive to active states (55). Transition between these two states is thought to be regulated by the binding of calcium to a "calcium sensor" (13, 38), but the identity and mechanism of the calcium sensor and the fusion complex is unknown. While binding of calcium to the sensor may be reversible, upon activation, a fusion complex can irreversibly commit to fuse (55). The sea urchin is a good preparation to study the calcium dependence of exocytosis because the fusion of predocked granules with the plasma membrane can be studied, in vitro, in the absence of reserve granule mobilization to docking sites, or in the absence of subsequent endocytotic activity.

The simplicity of cortical granule exocytosis in vitro allows the investigation of a feature common to almost every fusing system (28): submaximal response to calcium. We have recently concluded that sea urchin cortical granules are heterogeneous in their response to calcium (Kaplan, D., P.S. Blank, M.S. Cho, I. Steinberg, and J. Zimmerberg. *Biophys. J.* 66:A284 [Abstr.].). Depending only on calcium concentration, a cortical granule will either fuse in time or will never fuse, regardless of how long or the number of times calcium is applied. This striking behavior occurs even though all granules are docked. In this in vitro system docking has been characterized by EM (8, 61), and is functionally evident by the ability of granules to remain attached to the plasma membrane despite extensive perfusion (61). In this fusion system, it is not known if docking and membrane merger are mediated by the same components. In terms of the above description, a fusion complex is irreversibly activated when a threshold calcium concentration is exceeded, i.e., all conformational changes associated with the calcium sensor and the fusion complex that are required for membrane fusion to ensue are complete. We define this state as an activated fusion complex.

Practically all docked cortical granules fuse with the plasma membrane of in vitro preparations (4, 15, 51, 61) at calcium concentrations in excess of 100 μM (45, 52). This suggests that virtually all cortical granules have at least one fusion complex that can be activated by calcium. The total surface area of the granule (1-μm diameter; 8, 61) is 400 times the surface area of a 50-nm synaptic vesicle, so there is ample area on a cortical granule for more than one fusion complex. Docked cortical granules are derived from much smaller vesicles that bud from the Golgi (14), and in other systems, such precursor vesicles fuse to each other before plasma membrane docking (16, 17). If each precursor vesicle contained at least one fusion complex, then docked cortical granules would contain multiple complexes, which may concentrate at their docking sites.

Since fusion for a single granule is all-or-none, fusion can be caused by one activated fusion complex. After fu-

Please address all correspondence to Dr. S.S. Vogel, Building 10, Room 6C-215, 10 Center Drive, MSC 1855, National Institutes of Health, Bethesda, MD 20892-1855. Tel.: (301) 594-2658; Fax: (301) 594-0813; E-mail: Steven_Vogel@nih.gov

© The Rockefeller University Press, 0021-9525/96/07/329/10 $2.00

sion, the rest of the fusion complexes will be redundant, and will not contribute to either the extent or the rate of fusion. Thus, if exocytotic granules have multiple activated fusion complexes before fusion, their number and distribution can affect both the rate and extent of triggered exocytosis. Attempts to model the extents and kinetics of calcium-dependent fusion must consider the consequences of having multiple activated complexes. These consequences are examined in this study.

Materials and Methods

Cell surface complex (CSC)[1] was prepared and assayed for calcium-triggered exocytotic activity, as previously described (52). Sea urchin eggs were prepared from *Strongylocentrotus purpuratus* (Marinus, Long Beach, CA). Eggs in PKMEB (50 mM Pipes, 450 mM KCl, 10 mM $MgCl_2$, 5 mM EGTA, 1 mM BAPTA, 1 mM benzamidine, pH 6.7) at a ratio of 1:10 (vol/vol) were homogenized with 6–10 strokes of a Teflon-glass dounce homogenizer. The homogenate was centrifuged for 1 min at 200 *g* in a tabletop centrifuge. The pellet of CSC was resuspended in HENPK buffer (6 mM HEDTA, 6 mM EGTA, 3 mM NTA, 50 mM Pipes, 425 mM KCl, 1 mM benzamidine, pH 6.7) by gentle vortexing to form a turbid white solution.

Fusion complexes were fractionally inactivated by mixing CSCs with HENPK containing various concentrations of NEM (up to 20 mM) on ice. After the appropriate incubation time (up to 2 h), unreacted NEM was neutralized by the addition of 20 mM DTT. The calcium dependence of cortical granule fusion in CSCs was determined at room temperature using a turbidimetric microtiter dish assay, as previously described (52), and HENPK buffer containing defined calcium concentrations. Free calcium concentrations were measured for these buffers using a calcium electrode (World Precision Instruments, Inc., Sarasota, FL) or with the fluorescent calcium indicator BTC (Molecular Probes, Inc., Eugene, OR), whose fluorescence was measured using a CytoFluor 2350 fluorimeter (Millipore, Bedford, MA) with a ratio (R) of the light excited at 360 ± 40 and 485 ± 20 nm collected at 530 ± 25 nm. The free calcium concentration was calculated using the function $[Ca^{2+}] = K_d \times Q \times (R - R_{min})/(R_{max} - R)$ and an apparent K_d value of 73 ± 1 μM in HENPK buffer and a Q value of 6.6 ± 0.3.

Survival curves were measured by monitoring light scattering from planar isolated sea urchin egg cortices (61) that had been perfused with HENPK buffer containing defined concentrations of free calcium. Intact eggs were attached to polylysine-treated glass coverslips, and sheared with calcium-free HENPK buffer yielding a preparation consisting of exocytotic cortical granules docked on plasma membrane fragments attached to a glass coverslip. The coverslip was placed in a rapid perfusion chamber (25) and challenged with calcium buffers. In this chamber, buffer was completely replaced in <1 s. Light scattering was measured as previously described (61).

The fraction of refractile granules was measured using planar isolated sea urchin egg cortices (61). Granules were imaged using a Plan-Neofluar 63× 1.25 NA objective and Nomarski optics on an upright microscope (Carl Zeiss, Inc., Thornwood, NY). Cortices were incubated in a buffer containing 50 mM Pipes, 450 mM KCl, 1 mM benzamidine, 5 mM DM-nitrophen, and 2.5 mM $CaCl_2$, pH 6.7. Caged calcium was released from DM-nitrophen, as previously described (45). The number of granules present before and 1 min after opening the UV shutter was directly counted for 60 independent trials by four observers. The fraction of granules that failed to fuse was calculated, propagating sampling error. We only imaged centrally located regions of cortices to avoid edge problems (45).

The fate of randomly selected granules was followed once per second in intact *Lytechinus pictus* eggs, using differential interference video microscopy as described above. The noncensored Kaplan-Meier survival curve (31) for exocytosis was calculated from granule fusion times (Sigma Plot; Jandel Scientific, Corte Madera, CA).

Curve fitting was performed using the Levenberg-Marquardt algorithm, which minimizes the value of chi square. Igor Pro software (version 2.04; Wavemetrics, Inc., Lake Oswego, OR) was used to analyze the data. When error bars are shown, fits were weighted with the SD for each point to improve the estimates of the fitting coefficients. Error was propagated for all mathematical data transformations, as described by Bevington and Robinson (7).

1. *Abbreviations used in this paper*: BAPTA, bisaminophenoxy ethane -N, N, N′, N′ tetraacetic acid; CSC, cell surface complex; HEDTA, N- hydroxyethylethlendiamine triacetic acid; NTA, nitrilotriacetic acid.

Results

Models for Multiple Fusion Complexes

The active fusion complex is defined as the minimal set of components that can independently cause the fusion of a granule with the plasma membrane. We will consider two models that describe the rate and extent of fusion when the number of active fusion complexes on granules are varied, the fixed and random models. Assumptions common to both of these models are:

(*a*) All granules are predocked on the plasma membrane.
(*b*) Only active fusion complexes can initiate the fusion process.
(*c*) The transition between the inactive and active state is irreversible: granules with activated complexes are committed to fuse.
(*d*) The calcium concentration regulates the number of active fusion complexes.
(*e*) Upon activation, the probability in time that a fusion complex initiates the fusion process may be a function of the calcium concentration, but does not change with either time, the number of active fusion complexes, or the location of granules.
(*f*) Fusion complex activation is instantaneous relative to the time constant for observing fusion.

In addition to the above assumptions, there are two assumptions that are unique to either the fixed or random model. The fixed model assumes that every granule in a population will have a fixed integral number of active fusion complexes at any specific calcium concentration. In contrast, the random model assumes that active fusion complexes are randomly distributed between the granules in a population such that the total number of active fusion complexes is much greater than one, their average number per granule, and their number on any one granule.

Fixed Model

Triggered exocytosis of a population of granules can be treated as a survival process where the population of docked granules decreases by fusion. Let t = time in 1-s intervals, n = a fixed integer representing the number of active fusion complexes per granule, and p = the probability per second that an active fusion complex mediates a fusion event between a granule and the plasma membrane. The time dependence of exocytosis (survival) is:

$$S(t,n,p) = (1 - p)^{nt}$$

This formalism is the same as a coin toss problem. If granule fusion occurs on the first "heads" tossed, then p is equivalent to the probability per toss of getting a head, $(1 - p)$ is the probability of not getting a head, t is the toss turn number, and n is the number of coins tossed per turn. When p is not very large (<0.1), $S(t,n,p)$ decays exponentially with a time constant, np. If the parameters n or p are functions of $[Ca^{2+}]_i$, then increasing the value of either parameter would increase the rate of fusion. The rate of fusion is the derivative of $1 - S(t,n,p)$. A 0 value for either n

or p would result in no fusion, while all other values for n result in every vesicle fusing (Fig. 1). For example, if each granule has one active fusion complex, $n = 1$, and every granule fuses.

Random Model

If active fusion complexes are randomly distributed among a population of granules, then different granules can have different numbers of active fusion complexes, with t and p, as described above. $S(t,<n>,p)$ is the survival curve for a population containing individual granules that may have 0, 1, 2, 3, . . . active fusion complexes. The relative abundance of granules with different numbers of active fusion complexes is set by the value of $<n>$. Because we assume that large numbers of active fusion complexes are randomly distributed among large numbers of granules such that $<n>$ is small relative to the total number of active fusion complexes, $S(t,<n>,p)$ is the Poisson-weighted sum of individual, fixed model survival curves:

$$S(t,<n>,p) = \sum_{n=0}^{\infty} ((<n>^n/n!)\, e^{-<n>})\,(1-p)^{nt}$$
$$= e^{<n>((1-p)^t - 1)}$$

The maximal rate of fusion is the derivative of $1 - S(t,<n>,p)$ as t goes to 0:

$$R_{max} = -<n> \ln (1-p)$$

The extent of fusion, $E(<n>)$ is $1 - S(t, <n>, p)$ as t goes to infinity:

$$E(<n>) = 1 - e^{-<n>}$$

In the random model, increasing the value of either $<n>$ or p as a function of $[Ca^{2+}]_i$ would increase R_{max}. In contrast to the fixed model, random model survival curves are not single exponentials (at low values of p), but are weighted sums of exponentials. More importantly, survival curves do not always extrapolate to 0 (100% fusion), but can asymptotically approach intermediate values as t approaches infinity (Fig. 1): the extent of fusion, $1 - S(t \rightarrow \infty, <n>, p)$, is a function of $<n>$ alone.

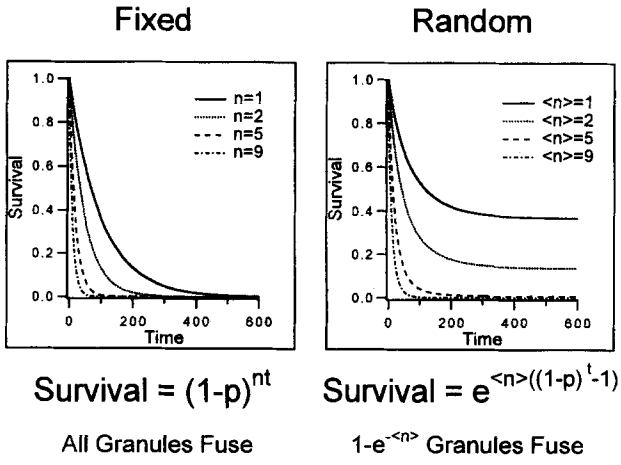

Figure 1. The dependence of survival on n, $<n>$, for the fixed model (*left panel*) and the random model (*right panel*). The value of p was constant ($p = 0.01$) and the values of n or $<n>$ were varied. In the random model, the presence of granules with no active fusion machines results in a fraction of granules that cannot fuse.

The Time Course of Exocytosis Can Be Fit by the Random Model

If active complexes are randomly distributed, and an increase in $[Ca^{2+}]_i$ corresponds to an increase in their number, then three predictions can be used to differentiate between these two models: (*a*) there should exist a range of calcium concentrations where submaximal extents of fusion are observed; (*b*) survival curves should be best fit by the random model; and (*c*) even at very high calcium concentrations (>1 mM), a small fraction of exocytotic granules should fail to fuse. In contrast, 100% should fuse if every granule has a fixed number of active fusion complexes (>0).

The extent of fusion was measured as a function of the calcium concentration in an in vitro preparation of sea urchin egg cortical granules that are predocked on isolated plasma membrane fragments. ATP, GTP, cytosol, and all other soluble factors were not included in the reaction mixture to obviate the possibility that calcium might, in addition to triggering fusion, also trigger fusion complex assembly. Consistent with the random model, submaximal extents of fusion were observed between 10 and 100 μM calcium (Fig. 2). To test the second prediction of the random model, survival curves were obtained from cortices that were exposed to either 16 or 350 μM calcium in a rapid perfusion chamber. At the lower calcium concentration, submaximal extents of fusion were observed, and the survival curve (Fig. 3 *A*) was well fit by the random model. This curve is poorly described by the fixed model, even when the constraint of noninteger n is lifted (compare residuals of best fits in Fig. 3 *A* and the error for the fitting parameters). At the higher calcium concentration, where the rate of fusion is much faster, the survival curve (Fig. 3 *B*) appears to be a convolution of the delivery of calcium (45), a calcium activation process (55), and the underlying fusion process. These additional kinetic processes preclude our use of this technique for obtaining accurate values of $<n>$ and p. Despite the convolution, a better fit was obtained when this survival curve was fit to the random model (see Fig. 3 *B*). The inability of the fixed model to fit either data set becomes even more apparent when the value of n is constrained to integer values. To test the last prediction of the random model, that even at high calcium concentrations a fraction of the granules ($e^{-<n>}$) fail to fuse, the fate of ~22,000 granules was determined after exposure to 2.5 mM calcium (see Fig. 4). Between 3–12 survivors were observed. This corresponded to a fusion efficiency >99.97% and to an $<n>$ value of 8.4 ± 0.6 (mean ± SEM; $n = 4$) in the random model. Since these predictions of the random model have been observed, it remains a viable description for the extent and rate of cortical granule exocytosis. In contrast, the fixed model is rejected.

Docking Sites Can Have on Average Nine Active Fusion Complexes

We reasoned that the maximum number of fusion complexes, on average, could be determined by randomly and irreversibly modifying the proteinaceous components of fusion complexes needed for their activity, and then measuring the extent of fusion in response to saturating concentrations of calcium. By definition, granules that fail to

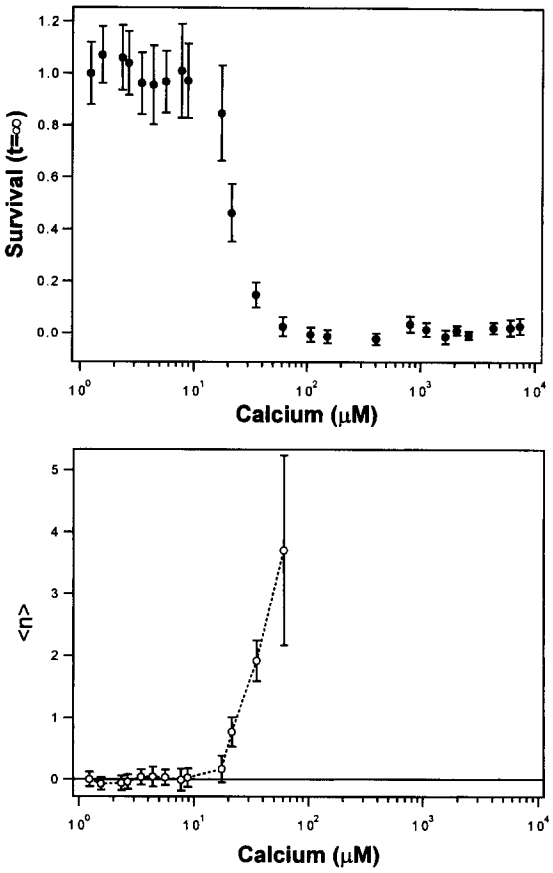

Figure 2. The top panel shows the calcium dependence of exocytosis in isolated cell surface complexes consisting of plasma membrane fragments and docked, ready releasable cortical granules. Points are mean ± SD, $n = 8$. Between 10 and 100 μM calcium, submaximal extents of exocytosis were observed. This behavior is consistent with the random model. The bottom panel shows the transformation of survival (S) into $<n>$ according to the relationship $<n> = -\ln(S)$, derived from the random model. As survival values approach 0, the error in $<n>$ increases. This is caused by our assay's inability to distinguish between 97 and 100% granule exocytosis. Below 10 μM calcium, granule exocytosis was not observed. Between 10 and 80 μM calcium, $<n>$ was proportional to pCa. The calcium dependence of $<n>$ above 80 μM was not measurable with this technique.

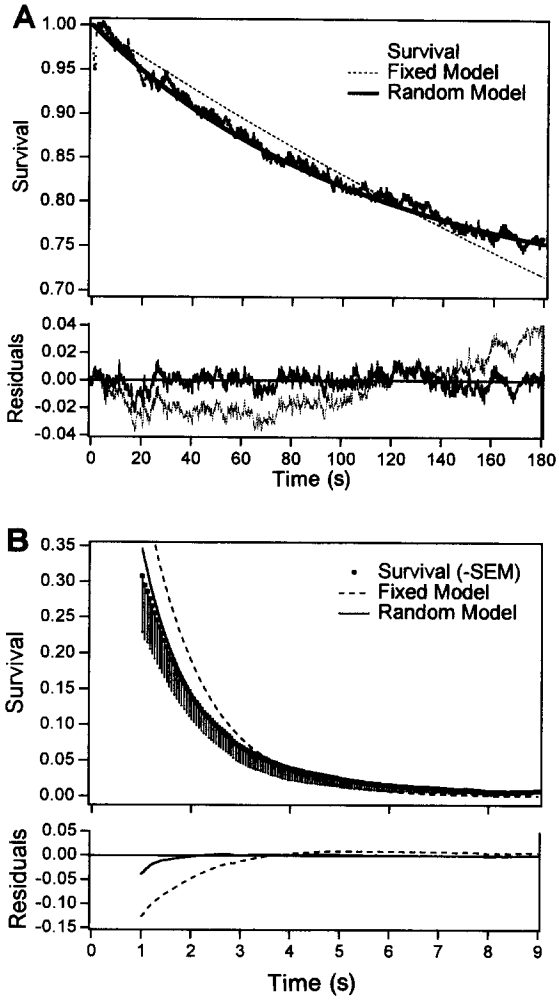

Figure 3. Survival curves for sea urchin egg cortices exposed to either 16 μm (A) or 350 μM (B) calcium. Cortices were perfused for 1 s with the calcium buffers beginning at $t = 0$. Survival curves were fit to either the fixed model or the random model, and residuals of the fits are plotted in the lower panels. The fitting parameters (±SE) for the fixed model in A were $n = 0.31 \pm 0.33$, $p = 0.006 \pm 0.006$, and the parameters for the random model were $<n> = 0.38 \pm 0.00$ and $p = 0.007 \pm 0.000$. (B) The fitting parameters for the fixed model were $n = 6.06 \pm 27.80$, $p = 0.129 \pm 0.549$, and the parameters for the random model were $<n> = 6.29 \pm 0.53$ and $p = 0.169 \pm 0.022$. Survival data in A was from a single experiment, while the survival curve in B is the mean (−SEM) from five experiments illustrating that both single and averaged data can be fit. The fits for average data in B were weighted by the sample variance.

fuse no longer have any active fusion complexes. NEM was chosen as an inhibitor because it is a known irreversible inhibitor of cortical granule exocytosis (15, 23). It is possible that the NEM-sensitive site in sea urchin eggs is related to the NSF protein that is involved in Golgi stack transfer, yeast secretion, and synaptic release (5, 12, 44). However, cortical granule exocytosis inhibited by NEM cannot be rescued by cytosol (58). Rather, NEM is thought to inhibit exocytosis by randomly modifying free sulfhydryls on fusion complex calcium sensors (58) residing on the exocytotic granules (53, 56). NEM treatment should progressively decrease the number of fusion complexes per granule, and the remaining complexes should be randomly distributed. If the average number of complexes is low and there are many granules studied at one time, then their distribution among granules is Poisson (7).

The Poisson distribution is a discrete frequency distribution of independent countable events which is completely characterized by a single parameter, the mean of the distri-

Figure 4. Four examples of exocytosis in response to 2.5 mM calcium from 60 individual experiments. Isolated sea urchin cortices were exposed to calcium before (*left*) and 1 min after (*right*). Occasionally, a granule failed to fuse in the presence of high calcium (see top video pair). Bar, 10 μm.

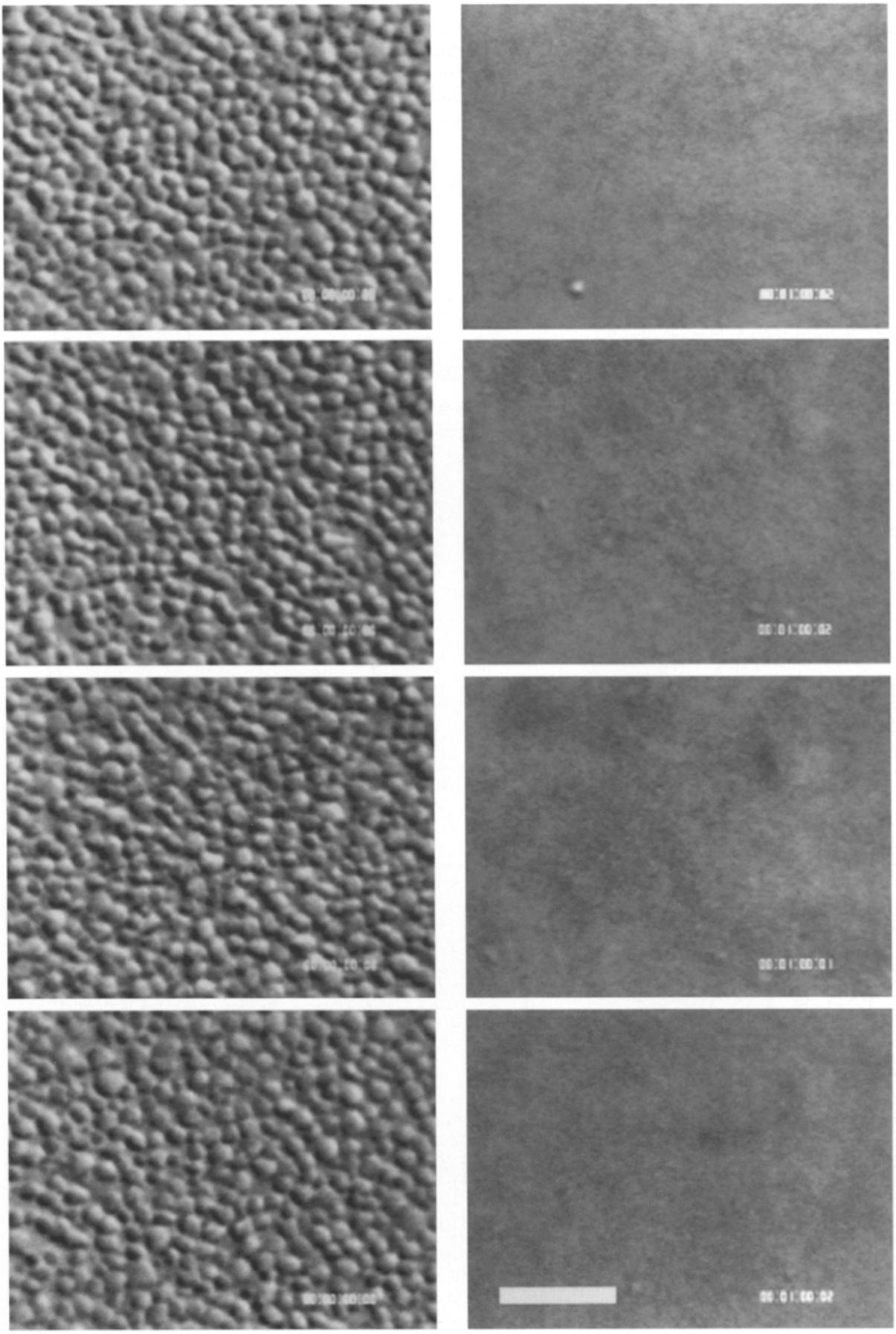

bution. The Poisson distribution describes many biological processes, such as the release of quanta at synaptic terminals (26). A population of granules with a Poisson distribution of active fusion complexes will have a fraction of granules ($e^{-<n>}$) with no active fusion complexes. By measuring the fraction, S, of granules in a population that survives after exposure to calcium, we can calculate the value of $<n>$ using the formula: $<n> = -\ln(S)$ (see Fig. 2). $<n>$ as a function of time of exposure to an inhibitor, or as a function of inhibitor concentration, enables extrapolation to the value of $<n>$ in an untreated cortex. The maximum number of active fusion complexes per granule, on average ($<n>_{MAX}$), can be measured at saturating calcium concentrations.

To measure the value of $<n>_{MAX}$, the calcium and NEM sensitivity of cortical granule exocytosis was characterized in isolated cell surface complexes consisting of plasma membrane fragments and docked, ready releasable cortical granules. Submaximal extents of exocytosis were observed between 10 and 100 μM calcium (Fig. 5). Granule exocytosis was not observed below 10 μM calcium. Mild NEM treatment shifted the survival activation curve, while more extensive treatment decreased the fraction of fusible granules. The decrease in the fraction of fusion competent granules could not be overcome with higher calcium concentrations (>1 mM). The plateau region observed above 1 mM calcium is consistent with the saturation of calcium sensor–binding sites: above 1 mM calcium additional active fusion complexes cannot be recruited. This calcium-NEM dose–response behavior is expected if calcium increases the value of $<n>$ while NEM treatment decreases $<n>$. This behavior is not unique to NEM, since treatment with proteases has the same effect (23). This classic pharmacological behavior, progressive shifting of a dose–response curve using mild treatments of irreversible inhibitors and the lowering of the extent of a reaction after harsher treatment, has been observed in tissue dose–response studies using irreversible competitive inhibitors (29, 41, 46), and is the hallmark of "receptor reserve" or "spare receptors" (32, 47).

The value of $<n>_{MAX}$ was determined by extrapolation of the concentration and time dependence of NEM inacti-

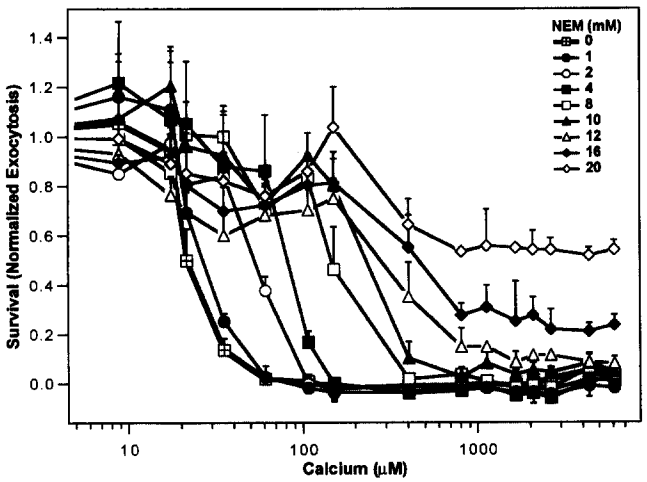

Figure 5. Mild NEM treatment shifts the survival activation curve, while more extensive treatment results in a decrease in the fraction of granules that are capable of fusing. CSCs were treated with different concentrations of NEM for 2 h on ice, and then a calcium dose response was measured using a turbidimetric assay. Points are mean + SD, $n = 3$.

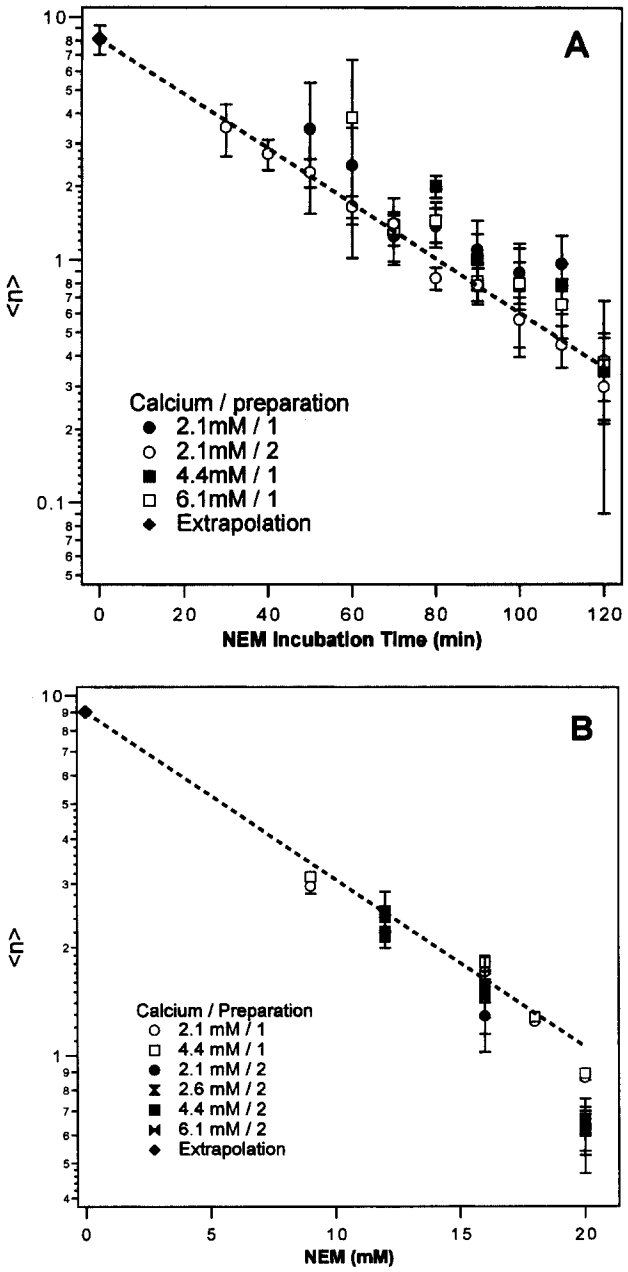

Figure 6. (*A* and *B*) The time and concentration dependence of the NEM inactivation of cortical granule survival after transformation into $<n>$. The decrease in $<n>$ is an exponential function of both the time of NEM inactivation or NEM concentration at the indicated calcium concentration. All experimental points are mean ± SD, $n = 3$. Dotted lines are weighted averages of all individual single exponential fits using the equation: $y = ae^{(-bx)}$, where a is a scaling parameter, b is either the time or concentration decay constant for NEM inactivation, and x is either the time or NEM concentration. The exponential extrapolation to either 0 NEM concentration or time 0 is mean ± SEM derived from individual fits and displayed on a log-linear plot to explicitly show the exponential nature of this process.

vation at calcium concentrations >1 mM. The decrease in $<n>$ is an exponential function of both the time of NEM treatment and the NEM concentration during a fixed time period (Fig. 6). A single exponential decay would be observed if fusion complex inactivation was both random and required either a single-site modification or modification of multiple identical sites. At all calcium concentrations measured, above 1 mM calcium $<n>_{MAX} = 9.0 \pm 0.2$ (mean ± 95% confidence) when extrapolated to a NEM concentration of 0, and $<n>_{MAX} = 8.1 \pm 2.2$ (mean ± 95% confidence) when extrapolated to time 0. These values of $<n>$ at high calcium concentrations are in agreement with the value of 8.4 ± 0.6 derived from the fraction of granules that failed to fuse at 2.5 mM calcium (Fig. 4). At lower concentrations of calcium (<1 mM), the extrapolated values of $<n>$ were lower. For example, at 809 μM calcium, $<n>$ had an extrapolated value of 6.0 ± 2.2 (mean ± SD).

We have demonstrated that at >1 mM calcium, $<n>$ reaches a maximum value of 9.0 ± 0.1 (mean ± SEM, n = 10). Below 1 mM calcium, the extent of fusion can be interpreted as the fractional activation of fusion complexes in response to calcium. Fig. 7 depicts the cumulative results of four techniques used to measure the calcium dependence of $<n>$ from sea urchin exocytotic preparations in vitro. No fusion was observed below 10 μM calcium, so $<n> = 0$. Between 10 and 800 μM calcium, $<n>$ increased with pCa. It is important to realize that 50% of granules fuse between 18 and 22 μM calcium, while in contrast, 50% of the fusion complexes, which can be activated, were active at ~100 μM calcium. These different half maximal calcium concentrations are derived, in part, from the same data set, and they illustrate the model dependence of assigning calcium-binding affinities.

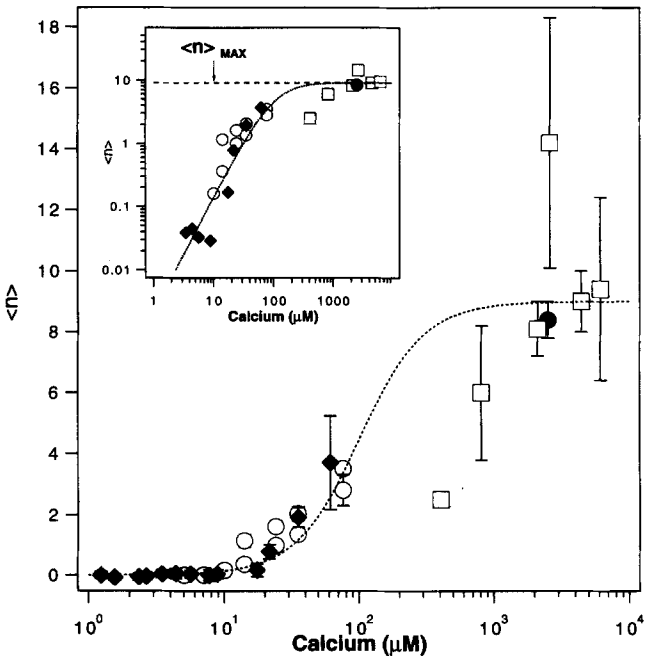

Figure 7. Four techniques were used to measure the calcium dependence of $<n>$ from sea urchin exocytotic preparations in vitro. The final extents from survival data for either CSCs (◆) or the perfused cortex (○) were transformed into $<n>$ values. At higher calcium concentrations where >98% of granules fuse, $<n>$ was measured either by extrapolation of NEM inactivation data (□), or by the number of refractile granules (●). The figure insert is the same data on a log-log scale.

To examine the applicability of the random model to describe the time course of exocytosis in intact cells, we visualized a population of cortical granules in *L. pictus* eggs during fertilization and measured the time course of exocytosis (Fig. 8, *A–C*). The exocytotic survival curve for this egg is shown in Fig. 8 *D*. After perfusion with sperm, there was a lag time during which sperm must find the egg, fuse with the oolemma, and release calcium from the egg's intracellular stores. Presumably, when the calcium concentration at docking sites reaches a threshold, granule fusion complexes are activated and mediate fusion with the plasma membrane. This survival curve can be parameterized by the random model (Fig. 8 *D*). In the egg, as observed in the isolated sea urchin egg cortex (Fig. 3 *B*), the initial portion of the survival curve (Fig. 8 *D*) may be convolved with the temporal and spatial characteristics of the calcium delivery and a calcium activation process. During fertilization, the subcortical space that was occupied by cortical granules before fusion (Fig. 8 *A*) is not invaded by cellular organelles in the cytoplasm after exocytosis (see Fig. 8 *C*).

Discussion

The Random Model

We envision cortical granule docking sites as having, depending upon $[Ca^{2+}]_i$, an average of between 0–9 active fusion complexes. Using the random model, we can rationalize much of the calcium-dependent exocytotic behavior observed in this preparation. These include (*a*) the sigmoidal dependence of survival on pCa due to the existence of submaximal responses (4, 60); (*b*) the increase in fusion rate with increase in $[Ca^{2+}]_i$ (10, 54); (*c*) the discrepancy between the calcium concentration required for maximal extents and rates (61); (*d*) shifting of the calcium activation curve with inhibitors of exocytosis (23, 34, 58); and (*e*) aging (45, 61), where a progressive decrease in calcium sensitivity is observed with time in the isolated planar cortex. The random model succeeds in describing all of these behaviors in the sea urchin with the simple hypothesis that an increase in $[Ca^{2+}]_i$ corresponds to an increase in the average number ($<n>$) and perhaps the efficacy (p) of active fusion complexes at docking sites. According to this model, the number of active fusion complexes per granule is a Poisson-distributed random variable, with a maximal average value of $<n> = 9$. In contrast, deterministic models such as the fixed model are not compatible with the data.

The random model links the rate and extent of degranulation, and can be used to fit the time dependence of exocytosis (Fig. 3). The fraction of granules that fuse at any calcium concentration is solely a function of one of these parameters, $<n>$, the average number of active fusion complexes at a docking site. Submaximal extents of fusion are observed because a fraction of granules containing no active fusion complexes will always exist when active fu-

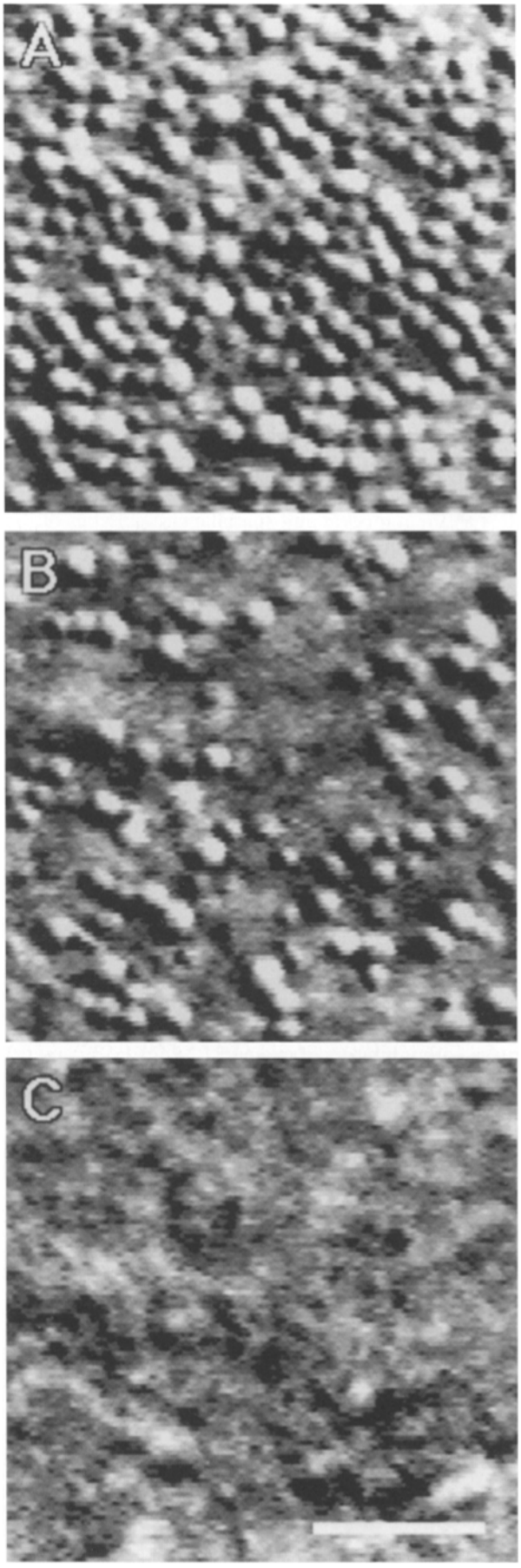

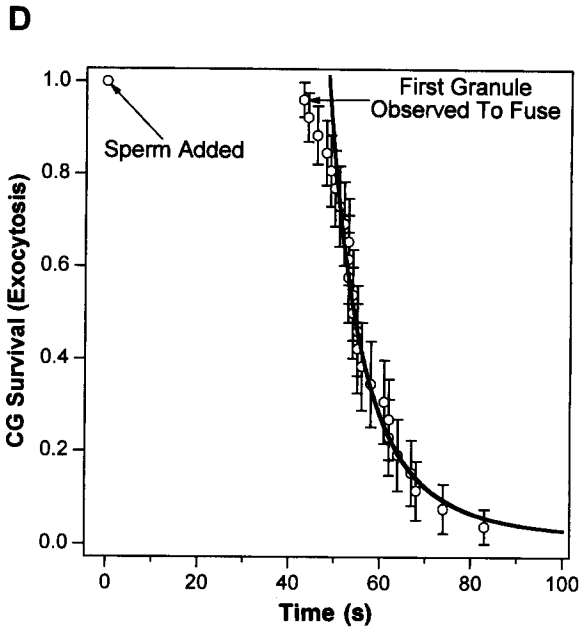

Figure 8. Cortical granule exocytosis observed in intact sea urchin eggs. Sea urchin eggs were perfused with a 1:1,000 dilution of sperm in artificial seawater at $t = 0$ s. (*A–C*) The subcortical space, normally occupied by cortical granules in the unfertilized egg, was imaged using differential interference video contrast microscopy at 40, 70, and 100 s after perfusion. The bar in *C* is 5 μm. The Kaplan-Meier survival data (○; mean ± SD) for sperm-triggered cortical granule exocytosis is shown in *D*. The solid line in *D* is a survival curve based on the random model ($S = e^{<n>((1-p)^{(t+\Delta t)}-1)}$) with $<n> = 4.5$, $p = 0.029$, and $\Delta t = -48.6$ s to allow for nonzero starting times.

sion complexes are randomly distributed. In the random model, the maximal rate of exocytosis is directly proportional to the average number of active fusion complexes: as $[Ca^{2+}]_i$ increases $<n>$, the maximal rate of exocytosis will increase. Since the extent of exocytosis is an asymptotic function of $<n>$ and the maximal rate is a linear function of $<n>$, they need not plateau at the same value of $<n>$. This differential dependence on $<n>$ can explain the difference in the calcium dependence of rate and extent observed in sea urchin eggs (61) and chromaffin cells (3). Since $<n>$ does plateau at >1 mM calcium, the maximal rate should also plateau at these concentrations. A plateau in the apparent maximal rate has been observed at >1 mM calcium in preliminary experiments (data not shown).

The random model does have limitations. In essence, the random model shifts the burden of explaining incomplete exocytosis to that of explaining incomplete conversion of inactive to active complexes. The nature of the coupling between calcium sensors and fusion complexes is not intrinsic to the model, nor is the assembly, activation, and other unknown aspects of producing a Poisson distribution of active fusion complexes. We can only speculate on issues such as the number and nature of calcium-binding sites, cooperativity between these sites, and the molecular mechanism for producing and maintaining Poisson-generated fusion complex heterogeneity. The origin of this be-

havior is under investigation. Fusion complexes which do not contact a target membrane may not be functional (55), and the model yields only the average number of functional complexes per granule. Thus, the number of 'functional' complexes may differ from the total number of complexes. Changes in the probability that a fusion complex initiates the fusion process have not been incorporated in this version of the model, nor have potential rate limiting steps, such as time dependent delivery of calcium or time dependent activation of fusion complexes. Indeed, there is evidence that fusion complexes are not "instantaneously" activated (61). This can be seen in the discrepancy between the initial time course of exocytosis and the initial time course generated using the random model (see Figs. 3 and 8). Finally, it is known that in vitro, granules adjacent to granules that have already fused are more likely to fuse themselves (45). This behavior might result from a local modification of n and p values on neighboring granules. This version of the model has not been modified to account for this.

Alternative Hypotheses

One might speculate that a granule-docking site contains a single fusion complex, but that the NEM-sensitive site resides on a factor required to assemble that complex in response to an increase in the calcium concentration. Because fusion complex assembly is thought to require ATP and other soluble proteins and factors (5, 44), and our assay was conducted in the absence of ATP, GTP, and all other soluble factors and proteins, this seems unlikely. Furthermore, cortical granule exocytosis in vitro has been observed within tens of milliseconds after calcium delivery (54); as it is thought in other systems (2), it is likely that only preassembled fusion complexes are functional.

By invoking schemes involving a single preassembled fusion complex at a docking site, it may be possible to explain some of the individual calcium-dependent behaviors associated with exocytosis. First, it is known that calcium increases the rate of fusion (10, 54) and NEM decreases the fusion rate (45). By invoking an intrinsic, time-dependent inactivation process, one can explain both submaximal extents of fusion and the shift in calcium dose–response observed with NEM treatment. However, there is no evidence for time-dependent inactivation in this system (45; Kaplan, D., P.S. Blank, M.S. Cho, I. Steinberg, and J. Zimmerberg. *Biophys. J.* 66:A284 [Abstr.].). Second, if progressive NEM treatment on a single fusion complex progressively shifts its calcium-binding constant until the complex is destroyed, one can explain why mild treatment with inhibitors shifts the calcium dependence of exocytosis and extensive treatment with inhibitors decreases the fraction of granules that fuse. However, in this scheme, the calcium dependence of rate and extent should be identical, contrary to our data (extent plateaus at ~100 μM, while rate plateaus at >1 mM calcium). Finally, any scheme having a single fusion machine per granule would require a cellular mechanism to enforce a one-granule–one-fusion complex distribution. No such mechanism has been described, and seems improbable when one considers the ontogeny of these large cortical granules.

In Vivo Application

The primary physiological role of cortical granule exocytosis is to prevent polyspermy (24), thus it is important that most of an egg's 15,000 cortical granules fuse within the first minute after sperm entry. An egg takes 9–10 s for 50% of the granules to fuse (35) in response to a calcium concentration estimated to reach between 150 and 170 μM (36). If we set random model parameters $<n> = 4.5$ and $p = 0.03$, 98.7% granule fusion will occur by 3 min with an apparent half-time of ~10 seconds, and at a maximum rate of ~2,000 granules fusing per second. An $<n>$ value of 4.5 requires that the calcium concentration at docking site reach ~100 μM, which is comparable to values reached at synapses (1, 33, 43). A maximum rate of 2,000 granules fusing per second is comparable to exocytotic rates observed in neuronal cells using capacitance techniques (3, 18). In the sea urchin egg, as in neuronal cells (6, 20, 42), calcium-triggered exocytosis is followed by endocytosis (59). Interestingly, docking sites that were occupied by cortical granules before fusion are not invaded by other exocytotic organelles located deeper in the cytoplasm when observed by differential interference contrast microscopy during the first few minutes after fertilization (see Fig. 8). This suggests that organelle access to the subcortical space is limited, consistent with the recent finding that newly formed endosomes occupy this space (59).

Spare Receptor System

It is well known that fractional occupation of receptors by ligand need not correspond directly to fractional biological response (41, 46), as in cells having spare receptors (29). This behavior has been reconstituted and studied in vitro (40). Activation of a single surface receptor may invoke maximal response despite the fact that most surface receptors are free to bind ligand. Apparently, this behavior can also be invoked in intracellular receptor-mediated systems, such as calcium-triggered exocytosis. Spare receptor mechanisms allow low affinity sites to mediate responses to low concentrations of ligand. More importantly, spare receptor systems may bring about a sharper dose response transition, comparable to cooperative ligand-binding transitions (30, 37). Thus, a biological switch with a sharp transition may be implemented by spare receptor system or strong positive cooperativity.

The calcium dependence of exocytosis has been studied in different cell types, as models for synaptic release (3, 9, 11, 18, 19, 21, 22, 27, 50, 57). We suggest that the rate and extent of calcium-triggered exocytosis at synapses may also be a function of the number, distribution, and efficacy of fusion complexes at docking sites, in addition to the speed, amplitude, and duration of calcium delivery to the exocytotic calcium sensor. It would be remarkable if Poisson analysis, which was essential for constructing the vesicular hypothesis for synaptic release (26), would now allow for the interpretation of its calcium dependence.

We thank Nadeem I. Shafi and Alfred Yergey for stimulating discussions; Drs. L. Chernomordik, J. Lippincott-Schwartz, A.V. Parsegian, and T. Whalley for critically reading our manuscript; and Myoung-Soon Cho for excellent technical assistance.

Received for publication 5 October 1995 and in revised form 2 May 1996.

References

1. Adler, E.M., G.J. Augustine, S.N. Duffy, and M.P. Charlton. 1991. Alien intracellular calcium chelators attenuate neurotransmitter release at the squid giant synapse. *J. Neurosci.* 11:1496–1507.
2. Almers, W. 1994. Synapses. How fast can you get? [news; comment]. *Nature (Lond.).* 367:682–683.
3. Augustine, G.J., and E. Neher. 1992. Calcium requirements for secretion in bovine chromaffin cells. *J. Physiol.* 450:247–271.
4. Baker, P.F., and M.J. Whitaker. 1978. Calcium-dependence of the cortical reaction in broken eggs of *Echinus esculentus* [proceedings]. *J. Physiol.* 284:50P–51P.
5. Bennett, M.K., and R.H. Scheller. 1994. A molecular description of synaptic vesicle membrane trafficking. *Annu. Rev. Biochem.* 63:63–100.
6. Betz, W.J., F. Mao, and G.S. Bewick. 1992. Activity-dependent fluorescent staining and destaining of living vertebrate motor nerve terminals. *J. Neurosci.* 12:363–375.
7. Bevington, P.R., and D.K. Robinson. 1992. Data Reduction and Error Analysis for the Physical Sciences. McGraw-Hill, Inc., New York. 328.
8. Chandler, D.E. 1984. Exocytosis in vitro: ultrastructure of the isolated sea urchin egg cortex as seen in platinum replicas. *J. Ultrastruct. Res.* 89:198–211.
9. Chow, R.H., J. Klingauf, and E. Neher. 1994. Time course of Ca^{2+} concentration triggering exocytosis in neuroendocrine cells. *Proc. Natl. Acad. Sci. USA.* 91:12765–12769.
10. Crabb, J.H., and R.C. Jackson. 1986. Polycation inhibition of exocytosis from sea urchin egg cortex. *J. Membr. Biol.* 91:85–96.
11. Douglas, W.W. 1974. Involvement of calcium in exocytosis and the exocytosis–vesiculation sequence. *Biochem. Soc. Symp.* 39:1–28.
12. Ferro-Novick, S., and R. Jahn. 1994. Vesicle fusion from yeast to man. *Nature (Lond.).* 370:191–193.
13. Geppert, M., Y. Goda, R.E. Hammer, C. Li, T.W. Rosahl, C.F. Stevens, and T.C. Sudhof. 1994. Synaptotagmin I: a major Ca^{2+} sensor for transmitter release at a central synapse. *Cell.* 79:717–727.
14. Guraya, S.S. 1982. Recent progress in the structure, origin, composition, and function of cortical granules in animal egg. *Int. Rev. Cytol.* 78:257–360.
15. Haggerty, J.G., and R.C. Jackson. 1983. Release of granule contents from sea urchin egg cortices. New assay procedures and inhibition by sulfhydryl-modifying reagents. *J. Biol. Chem.* 258:1819–1825.
16. Hammel, I., D. Lagunoff, and P.G. Kruger. 1988. Studies on the growth of mast cells in rats. Changes in granule size between 1 and 6 months. *Lab. Invest.* 59:549–554.
17. Hammel, I., D. Lagunoff, and R. Wysolmerski. 1993. Theoretical considerations on the formation of secretory granules in the rat pancreas. *Exp. Cell Res.* 204:1–5.
18. Heidelberger, R., C. Heinemann, E. Neher, and G. Matthews. 1994. Calcium dependence of the rate of exocytosis in a synaptic terminal. *Nature (Lond.).* 371:513–515.
19. Heinemann, C., L. von Ruden, R.H. Chow, and E. Neher. 1993. A two-step model of secretion control in neuroendocrine cells. *Pflugers Arch.* 424: 105–112.
20. Heuser, J.E., and T.S. Reese. 1981. Structural changes after transmitter release at the frog neuromuscular junction. *J. Cell Biol.* 88:564–580.
21. Holz, R.W., M.A. Bittner, S.C. Peppers, R.A. Senter, and D.A. Eberhard. 1989. MgATP-independent and MgATP-dependent exocytosis. Evidence that MgATP primes adrenal chromaffin cells to undergo exocytosis. *J. Biol. Chem.* 264:5412–5419.
22. Horrigan, F.T., and R.J. Bookman. 1994. Releasable pools and the kinetics of exocytosis in adrenal chromaffin cells. *Neuron.* 13:1119–1129.
23. Jackson, R.C., K.K. Ward, and J.G. Haggerty. 1985. Mild proteolytic digestion restores exocytotic activity to *N*-ethylmaleimide–inactivated cell surface complex from sea urchin eggs. *J. Cell Biol.* 101:6–11.
24. Jaffe, L.A., and N.L. Cross. 1986. Electrical regulation of sperm-egg fusion. *Annu. Rev. Physiol.* 48:191–200.
25. Kaplan, D., J. Zimmerberg, A. Puri, D.P. Sarkar, and R. Blumenthal. 1991. Single cell fusion events induced by influenza hemagglutinin: studies with rapid-flow, quantitative fluorescence microscopy. *Exp. Cell Res.* 195:137–144.
26. Katz, B. 1971. Quantal mechanism of neural transmitter release. *Science (Wash. DC).* 173:123–126.
27. Knight, D.E., and P.F. Baker. 1982. Calcium-dependence of catecholamine release from bovine adrenal medullary cells after exposure to intense electric fields. *J. Membr. Biol.* 68:107–140.
28. Knight, D.E., and P.F. Baker. 1987. Exocytosis from the vesicle viewpoint: an overview. *Ann. NY Acad. Sci.* 493:504–523.
29. Kono, T., and F.W. Barham. 1971. The relationship between the insulin-binding capacity of fat cells and the cellular response to insulin. Studies with intact and trypsin-treated fat cells. *J. Biol. Chem.* 246:6210–6216.
30. Koshland, D., Jr., G. Nemethy, and D. Filmer. 1966. Comparison of experimental binding data and theoretical models in proteins containing subunits. *Biochemistry.* 5:365–385.
31. Lee, E.T. 1992. Statistical methods for survival data analysis. *In* Wiley series in probability and mathematical statistics. Applied probability and statistics. John Wiley & Sons, New York. 482.
32. Limbird, L.E. 1986. Cell surface receptors: a short course on theory and methods. Martinus Nijhoff Publishing, Boston. 196.
33. Llinas, R., M. Sugimori, and R.B. Silver. 1992. Microdomains of high calcium concentration in a presynaptic terminal. *Science (Wash. DC).* 256: 677–679.
34. McLaughlin, S., and M. Whitaker. 1988. Cations that alter surface potentials of lipid bilayers increase the calcium requirement for exocytosis in sea urchin eggs. *J. Physiol.* 396:189–204.
35. Mohri, T., and Y. Hamaguchi. 1990. Quantitative analysis of the process and propagation of cortical granule breakdown in sea urchin eggs. *Cell Struct. Funct.* 15:309–315.
36. Mohri, T., and Y. Hamaguchi. 1991. Propagation of transient Ca^{2+} increase in sea urchin eggs upon fertilization and its regulation by microinjecting EGTA solution. *Cell Struct. Funct.* 16:157–165.
37. Monod, J., J. Wyman, and J.P. Changeux. 1965. On the nature of allosteric transitions: a plausible model. *J. Mol. Biol.* 12:88–118.
38. Neher, E., and R. Penner. 1994. Mice sans synaptotagmin [news]. *Nature (Lond.).* 372:316–317.
39. Neher, E., and R.S. Zucker. 1993. Multiple calcium-dependent processes related to secretion in bovine chromaffin cells. *Neuron.* 10:21–30.
40. Neubig, R.R., and J.B. Cohen. 1980. Permeability control by cholinergic receptors in Torpedo postsynaptic membranes: agonist dose-response relations measured at second and millisecond times. *Biochemistry.* 19:2770–2779.
41. Nickerson, M. 1956. Receptor occupancy and tissue response. *Nature (Lond.).* 178:697–698.
42. Nordmann, J.J., P.F. Baker, M. Ravazzola, and F. Malaisse-Lagae. 1974. Secretion-dependent uptake of extracellular fluid by the rat neurohypophysis. *Nature (Lond.).* 250:155–157.
43. Roberts, W.M., R.A. Jacobs, and A.J. Hudspeth. 1990. Colocalization of ion channels involved in frequency selectivity and synaptic transmission at presynaptic active zones of hair cells. *J. Neurosci.* 10:3664–3684.
44. Rothman, J.E. 1994. Mechanisms of intracellular protein transport. *Nature (Lond).* 372:55–63.
45. Shafi, N.I., S.S. Vogel, and J. Zimmerberg. 1994. Using caged calcium to study sea urchin egg cortical granule exocytosis in vitro. *Methods: A Companion to Methods in Enzymology.* 6:82–92.
46. Stephenson, R.P. 1956. A modification of receptor theory. *Br. J. Pharmacol.* 11:379–393.
47. Taylor, P., and P.A. Insel. 1990. Molecular basis of pharmacologic selectivity. *In* Principles of Drug Action: The Basis of Pharmacology. W.B. Pratt and P. Taylor, editors. Churchill Livingstone Inc., New York.
48. Thomas, P., A.K. Lee, J.G. Wong, and W. Almers. 1994. A triggered mechanism retrieves membrane in seconds after $Ca^{(2+)}$-stimulated exocytosis in single pituitary cells. *J. Cell Biol.* 124:667–675.
49. Thomas, P., A. Surprenant, and W. Almers. 1990. Cytosolic Ca^{2+}, exocytosis, and endocytosis in single melanotrophs of the rat pituitary. *Neuron.* 5: 723–733.
50. Thomas, P., J.G. Wong, A.K. Lee, and W. Almers. 1993. A low affinity Ca^{2+} receptor controls the final steps in peptide secretion from pituitary melanotrophs. *Neuron.* 11:93–104.
51. Vacquier, V.D. 1975. The isolation of intact cortical granules from sea urchin eggs: calcium ions trigger granule discharge. *Dev. Biol.* 43:62–74.
52. Vogel, S.S., S. Beushausen, and D.S. Lester. 1995. Application of a membrane-fusion assay for rapid drug screening. *Pharm. Res.* 12:1417–1422.
53. Vogel, S.S., L.V. Chernomordik, and J. Zimmerberg. 1992. Calcium-triggered fusion of exocytotic granules requires proteins in only one membrane. *J. Biol. Chem.* 267:25640–25643.
54. Vogel, S.S., K. Delaney, and J. Zimmerberg. 1991. The sea urchin cortical reaction. A model system for studying the final steps of calcium-triggered vesicle fusion. *Ann. NY Acad. Sci.* 635:35–44.
55. Vogel, S.S., E.A. Leikina, and L.V. Chernomordik. 1993. Lysophosphatidylcholine reversibly arrests exocytosis and viral fusion at a stage between triggering and membrane merger. *J. Biol. Chem.* 268:25764–25768.
56. Vogel, S.S., and J. Zimmerberg. 1992. Proteins on exocytic vesicles mediate calcium-triggered fusion. *Proc. Natl. Acad. Sci. USA.* 89:4749–4753.
57. von Ruden, L., and E. Neher. 1993. A Ca-dependent early step in the release of catecholamines from adrenal chromaffin cells. *Science (Wash. DC).* 262:1061–1065.
58. Whalley, T., and A. Sokollof. 1994. The *N*-ethylmaleimide-sensitive protein thiol groups necessary for sea urchin egg cortical granule exocytosis are highly exposed to the medium and are required for triggering by Ca^{2+}. *Biochem. J.* 302:391–396.
59. Whalley, T., M. Terasaki, M.S. Cho, and S.S. Vogel. 1995. Direct membrane retrieval into large vesicles following exocytosis in sea urchin eggs. *J. Cell Biol.* 131:1183–1192.
60. Whitaker, M.J., and P.F. Baker. 1983. Calcium-dependent exocytosis in an in vitro secretory granule plasma membrane preparation from sea urchin eggs and the effects of some inhibitors of cytoskeletal function. *Proc. R Soc. Lond. B Biol. Sci.* 218:397–413.
61. Zimmerberg, J., C. Sardet, and D. Epel. 1985. Exocytosis of sea urchin egg cortical vesicles in vitro is retarded by hyperosmotic sucrose: kinetics of fusion monitored by quantitative light-scattering microscopy. *J. Cell Biol.* 101:2398–2410.